Adaptive Time-Frequency Synthesis for Waveform Discernment in Wireless Communications

Steve Chan
Vit Tall and University of Arizona
Orlando, USA
schan@vittall.org

Marwan Krunz
University of Arizona
Tucson, USA
krunz@arizona.edu

Bob Griffin
University of Arizona
Tucson, USA
bobgriffin@me.com

Abstract*—The discernment of waveforms for the purpose of identifying the underlying wireless technologies and validating if observed transmissions are legitimate or not remains a challenge within the communications sector and beyond. Conventional techniques struggle to robustly process Signals under Test (SuTs) in real-time. A particular difficulty relates to the selection of an appropriate window size for the processed data when pertinent contextual information on SuTs is not known a priori. The disadvantage of applying a predetermined fixed window size is that of length and shape (i.e., coarse resolution). In contrast, an *adaptive* window size offers more optimally tuned resolution. Towards this end, we propose a novel approach that uses an *Adaptive Resolution Transform* (ART) to either maintain a constant (prespecified) resolution, via a Variable Window Size and Shape (VWSS), or adjust the resolution (again using the VWSS technique) to match latency requirements. Central to this approach is the utilization of Continuous Wavelet Transforms (CWTs), which do not substantively suffer from those energy leakage issues found in more commonly used transforms such as Discrete Wavelet Transforms (DWT). A robust numerical implementation of CWTs is presented via a particular class of Convolutional Neural Networks (CNNs) called Robust Convex Relaxation (RCR)-based Convolutional Long Short-Term Memory Deep Neural Networks (a.k.a., CLSTMDNNs or CLNNs). By employing small convolutional filters, this class leverages deeper cascade learning, which nicely emulates CWTs. In addition to its use for convex relaxation adversarial training, the RCR framework also improves the bound tightening for the successive convolutional layers (which contain the cascading of ever smaller "CWT-like" convolutional filters). In this paper, we explore this particular architecture for its discernment capability among the SuT time series being compared. To operationalize this architectural paradigm, non-conventional Nonnegative Matrix Factorization (NMF) and Multiresolution Matrix Factorization (MMF) is used in conjunction to facilitate the capture of the structure and content of the involved matrices so as to achieve higher resolution and enhanced discernment accuracy. The desired WT (a.k.a., Corresponding WT or CORWT) resulting from the MMF is implemented as a translation-invariant CWT PyWavelet to better illuminate the intricate structural characteristics of the SuT and facilitate the analysis/discernment of their constituent Waveforms of Interest (WoIs). A pre-computed hash and lookup table is utilized to facilitate WoI classification and discernment in quasi-real-time.

Keywords—Waveform discernment, signal classification, convolutional long short-term memory deep neural network, robust convex relaxation, mimicked signals, real-time spectral analysis, window weighting function.

I. Introduction

Waveform discernment plays an important role in complex wireless environments. It endeavors to identify the underlying wireless technologies in a spectrum sharing scenario, e.g., Wi-Fi/Long Term Evolution (LTE)/Fifth Generation (5G) sharing of the unlicensed 5/6 GHz bands [1], LTE/radar coexistence over the Citizens Broadband Radio Service (CBRS) band, etc. It also endeavors to identify the types of Radio Frequency (RF) interference over a channel. Certain exogeneous interference may be caused by benign spurious emissions; others may induce strong (albeit unintentional) interference. Yet some RF transmissions may be malicious, aiming to disrupt ongoing communications. To further complicate matters, "mimics" of valid waveforms may also be synthesized for the purpose of deceiving intended receivers and signal classifiers [2]. In mission-critical domains, such as secure military communications and autonomous vehicles, the ability to discern between valid and altered waveforms is central. A successful approach to this problem space should have a profound impact across not only these sectors (i.e., communications, autonomous systems), but also other critical infrastructure sectors (e.g., energy).

Recently, many of the core functions needed to process SuTs and discern among their underlying WoIs have been modified/corrected to achieve more accurate and precise results; a sampling of the involved issues/bugs within various libraries, toolkits, and frameworks (e.g., Caffe, Caffe2, Julia, PyTorch, SciPy, TensorFlow, etc.) was delineated in [3]. The affected functions included, among others, Fast Fourier Transform (FFT), Inverse FFT (IFFT), Real-Valued FFT (RFFT), Inverse RFFT (IRFFT), Short-Time Fourier Transform (STFT), and Inverse STFT (ISTFT). By achieving sufficient precision (via resolution of the delineated issues/bugs) and the subsequent advent of more robust functions, the derived frequency-to-time mappings of WoIs are now potentially much more meaningful, particularly in the realm of 5G/B5G/6G waveform discernment.

Historically, spectrum analyzers that exhibit a high dynamic range have been utilized to analyze SuTs. However, waveform discernment in the frequency domain had limited success, as it has not been possible to recover exact time-domain amplitudes of the SuTs, which are approximated/averaged during the computational process. The limitations are exacerbated when the SuT is wideband, changing rapidly with time, or when pronounced differentiators appear at the higher-order harmonics. Various hybridized approaches have also been proposed, but have met with limited success. For example, the

often-utilized STFT-based method of converting SuTs from the time domain to the time–frequency domain has the disadvantage of having a fixed window size [4, 5]. Specifically, a narrow window $w[i]$, where i is the index of a time interval, might truncate and heuristically weight the SuT $S[i]$ so as to produce a distorted representation $dr[i]= S[i]\cdot w[i]$. On the other hand, an overly-wide window might introduce overlapping issues; these overlapping issues preclude the leveraging of natural inverses (which can facilitate the design of optimized inverses), at the temporal gaps between windows, which might better constrain the spread of time-frequency domain artifacts. Typically, a wider window provides a higher frequency resolution but lower time resolution, and vice versa. The limitations of a fixed window size reside not only in its predetermined dimensions but also its shape; the impact of shape is profound, as the artifact of spectral leakage can actually be somewhat controlled/mitigated by adjusting the shape of the window. Therefore, it should be of no surprise that the various approaches involving a fixed window size, such as experiments involving wide windows for higher frequency resolution and narrow windows for higher time-frequency resolution, have both, thus far, fallen short of achieving the requirements of robust SuT analysis.

To meet the aforementioned challenge, several STFT alternatives have been tried, including WT-based approaches [6]. Some studies describe how to bridge the gap between STFT and WT by deriving a transform that can be expressed as a variant of the STFT and, by way of example, as a discretization of the CWT [7]. Of significance, the WT of a lower-dimensional SuT results in a higher-dimensional *scaleogram* (a spectrogram generated by a WT), which can then provide insight into not only the period of, say, the largest oscillations, but also when these oscillations occurred. In addition to providing insight into the dynamic behavior of the SuT, scaleograms can also be utilized to discern among different SuTs and their constituent WoIs. The differences among the involved scaleograms equate to variations among the time series being compared, and CWT is preferred, as it is most suited for time series analysis due to its enhanced resolution and singularity illumination.

The preference of CWT over DWT is not limited to reasons of resolution alone. Spectral leakage is an inherent deficiency of DWT, which is subject to fixed windowing and limited sampling. An extension of the DWT, the Stationary Wavelet Transform (SWT) does not suffer from the spectral leakage problem, and it has a time-invariant property that somewhat preserves time-frequency characteristics through various levels of decomposition [8]. However, SWT tends to overcompensate (i.e., overdetermined) and often results in a redundant representation (hence, it is often referred to as the Redundant Wavelet Transform) of the original SuT. For these reasons, CWT is still the preferred WT embodiment.

This paper argues that it is possible to achieve meaningful waveform discernment through a specific logical progression: (1) transforming a lower-dimensional SuT to a higher-dimensional scaleogram (ideal for discerning variations among time series), (2) utilizing CWT (ideal for its enhanced resolution and singularity) for the time series analysis, (3) deriving CWT from a unique NMF/MMF amalgam (ideal for a Valid Generative Model or VGM [i.e., a probabilistic model of the input] approach), (4) implementing the desired ART/translation-invariant CWT PyWavelet schema via cascading, smaller convolutional filters aboard a RCR-based CLNN (ideal for its bound tightening) to better discern the constituent WoIs of the original SuT, and (5) leveraging a pre-computed hash and lookup table for undertaking WoI classification/discernment in quasi-real-time. The novelty of the approach resides in the sequence/implementation of the transformations.

The remainder of this paper is organized as follows. Section II discusses some of the waveform discernment challenges/limitations. Section III presents our approach for a robust waveform discernment system. Section IV features some of our experimentation findings, and Section V concludes the paper and outlines future work.

II. Waveform Discernment Challenges

Waveform discernment has been applied in many disciplines (e.g., monitoring of industrial control systems, electric machines, etc.) for the purpose of detecting and isolating certain distinguishing aspects [9]. In the wireless domain, waveform discernment is used to classify WoIs that are generated by heterogeneous technologies (i.e., non-compatible, but coexisting) that share a given spectrum. To date, the challenge of developing mechanisms to achieve robust waveform discernment has been non-trivial, particularly when it pertains to attribution of the involved WoI (and its encompassing SuT), without decoding it, to one of several possible technologies, interference sources, and/or mimic sources (if applicable) [1]. Some of these challenges/limitations are discussed next.

A. Limitations of FFT and DFT

The classification of WoIs typically involves the processing of a SuT into its constituent WoIs and the decomposition of the WoIs into their constituent frequency components (such as by Fourier Transform or FT analysis). FT can be implemented, by way of example, as FFT or DFT. FFT is computationally faster than DFT, but it is constrained by the range (in contradistinction to size, which refers to the number of constituent bins utilized for dividing the involved window into equal segments) of data that can be transformed, which begets the need for a Window Weighting Function (WWF) — a smoothing window function that compensates for the "spectral leakage." This leakage is due to windowing constraints of the data, and specifically the feeding of a non-integer number of cycles of the SuT to the FFT [10]. As the non-integer cycle frequency component of the SuT does not nicely correspond to spectrum frequency lines, in essence, the associated spectral leakage distorts the SuT measurement in such a way that energy from a given frequency component can "leak" or spread to the full bandwidth (i.e., across the various frequency lines and intervals or bins) [11]. This phenomenon is sometimes referred to as *spectral smearing* [12].

In contrast, DFT is not constrained by the range of data to be transformed (i.e., accommodates precise definition of the range over which to transform); hence, a WWF is not necessary. After applying DFT, by way of example, Spectral Analysis (SA) can be conducted to identify, in real-time, the frequency

spectrum of fast rare/transient events [13]; however, a robust literature review affirms that, in many cases, the involved DSP "is inefficient at performing the requisite Real-Time Spectrum Analysis (RT-SA) over instantaneous frequency bandwidths above the sub-GHz range" or for tracking "spectral changes faster than a few microseconds" [14]. Clearly, this is a concern for 5G/B5G/6G systems given that a significant portion of their spectrum lies in the high-bands (24 to 53 GHz).

B. Limitations of DSP-based RT-SA and Time-Mapped FT

To aggravate matters, the intrinsic limitations of DSPs further degrade the resolution (e.g., blindspots, signal loss, etc.) of the aforementioned approaches. For example, due to the performance (e.g., speed) limitations of typical DSP engines, conventional approaches often leverage frequency-to-time mappings that enable RT-SA of short, isolated pulse-like signals; however, these approaches are not able to robustly handle non-pulse-like (i.e., continuous) signals. Hence, conventional DSP-based RT-SA approaches are limited to sub-GHz bandwidths (e.g., < 500 MHz) and cannot readily intercept transients that are faster than a few microseconds. This begets the need for an approach vector that can achieve more robust RT-SA, particularly for wideband waveforms, in a continuous and gap-free fashion [14]. Of the various approaches utilized to address this problem, Time-Mapped FT (TM-FT) had been asserted to have promise. TM-FT maps the incoming SuT along the time domain (i.e., frequency-to-time mapping), and in a dispersion approach, different frequency components of the SuT travel at different speeds such that each spectral component can be mapped to a distinct and disparate time delay with a resultant TM-FT. This approach enables the capture of broadband spectral information, which includes the desired fast rare/transient events.

Yet, according to [14], TM-FT is inherently constrained to implementing the static FT of a pulse-like waveform, in such a way that consecutive pulses (e.g., with changing spectra) must be temporally separated by a gap much longer than the pulse duration; consequently, in the most general case of continuous waveform analysis, the utilization of TM-FT will result in the SuT being truncated (as well as various downstream distortions due to SuT truncation-related miscalculations) along the time axis, leading to the loss of a substantial portion of the signal information that resides between consecutive truncated signal sections. For a conventional implementation of the method, it has been asserted that enabling FT with a number of points of ~10 incurs a signal loss of over 90% [14].

III. Posited Approach to address the Challenge

The authors in [13] presented experiments involving Fourier SA of highly time-varying waveforms with results of GHz-bandwidth spectrograms (the SuT was captured at a speed of $\sim 5\times10^9$ FTs per second with ~5 ns duration frequency transients). From a technical perspective, they utilized a "combination of temporal sampling and dispersive delay so as to effectuate a 'virtual' temporal windowing of the input SuT" (i.e., Successive Analysis Windows or SAWs) and "subsequent FT computation without the need to implement an actual high-speed time truncation" of the incoming SuT [13]. This was performed in such a way that the SAWs nicely overlap, thereby mitigating against signal loss (i.e., gap-free operation). To expound upon this, and as a fork from this prior work, this paper focused upon STFT as a starting point and moved beyond prototypical STFT approaches. Axiomatically, this would have a distinct advantage over the deficiency of FT (which can achieve high resolution in the frequency-domain, but not necessarily in the time-domain).

By way of background information, prototypical STFT approaches utilize fixed-size time-shifted windows functions *w(i)* to obtain a transformation of the SuT, and ideally, the desired resolution is achievable given suitable splitting of various parts of a fixed size. However, this process introduces uncertainty, so it should be of no surprise that prototypical STFT approaches are deemed to have medium resolution in both the frequency and time domain. Moreover, prototypical STFT approaches are best suited for non-stationary data (which is not the case for SuTs). Hence, generally speaking, prototypical STFT approaches are construed to be fixed and single resolution approach. In reality, contending with SuTs requires a dynamic multi-resolution capability. Accordingly, approaches beyond prototypical STFT are needed.

To achieve this, it is necessary to progress beyond prototypical implementations of STFT; many of these implementations (e.g., TensorFlow, SciPy, as well as other libraries/platforms, such as SciPy) can introduce variances that may have a profound impact on any ensuing processing and phase analysis [15]. Our chosen implementation, which has promise, involved Nonnegative Matrix Factorization (NMF) of the spectrogram of an STFT conjoined with Multiresolution Matrix Factorization (MMF); these implementation components are described in Sections IIIA and B next.

A. NMF of the Spectrogram of an STFT

The ability to discern from among spectrograms is a lynchpin of the overarching posited approach. Prior research has been conducted regarding the NMF of spectrograms. NMF has become a prevalent unsupervised learning approach for the analysis of high-dimensional data, as it can facilitate feature extraction from very large sparse matrices [16], whereas existing algorithms are not readily able to process very large matrices due to various issues, such as missing entries or prolonged convergence. By way of example, let us take the case wherein a very large matrix A is factorized into, say, matrices B and C; the desire is that all the involved matrices have no negative elements [17]. However, if a prototypical method of matrix factorization, such as Singular Value Decomposition (SVD) is used, the resulting SVD-based low rank representation leads to images of both positive and negative elements (thereby violating the desire to have no negative elements), which makes interpretation difficult due to the *ambiguity*. In sharp contrast, NMF has the constraint that the factorized matrices have non-negative (i.e., positive) elements. Hence, NMF-based factorization facilitates a more robust interpretation of the original matrix data, as it articulates a clear and logical *representation by parts*. After all, the involved approximation/representation as the sum of positive elements (e.g., matrices, vectors, integers) is *logical and natural* (a.k.a., *naturalistic*) since images are simply matrices of positive integers representing pixel intensities. By leveraging

the advantage of NMF's non-negative element constraint, the high-level features of the spectrogram are more readily extracted from the interior layers (a.k.a., hidden layers) of the neural network, as the NMF-based approach is more *naturalistic* and reduces the need for feature engineering (i.e., a coarser approach of extraction). As the utilized CLNN architecture is already underpinned by a "white box" RCR approach (i.e., RCR-based CLNN) as discussed in [3], NMF can further facilitate the resultant outputs being more readily explained.

B. SuT Synthesis Model (SSM) as a Non-Conventional NFM Approach, for Facilitating MMF

STFT often serves as input to the NMF algorithm [18]. While prototypical NMF approaches are not able to provide a VGM of the STFT itself, the Gaussian Composite Model (GCM) is a VGM of the STFT and is depicted in Equation 1 [19],

$$y_{fn} \sim N_c\big(0, [WH]_{fn}\big), \tag{1}$$

where y_{fn} denotes the complex-valued coefficients of the STFT of the SuT, f denotes the index frequencies, n denotes the time frames, and N_c denotes a subclass often used in signal processing — the circularly-symmetric complex normal (a.k.a., complex normal) that corresponds to the zero-relation matrix — wherein zero denotes $\mu = 0$ and $C = 0$. Yet, while the GCM constitutes a generative model of the STFT, it is not yet a generative model of the raw SuT. In essence, it is still a proxy SuT Synthesis Model (SSM). Other operations fully transform the GCM to a fully formed SSM, which then segues to the MMF, its Corresponding WT (CORWT), and the resultant CWT. The described transformation progression is shown in Figure 1.

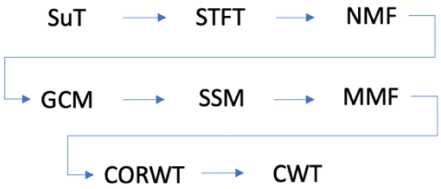

Fig. 1. Transformation of raw SuT to CWT.

To operationalize the transformation process, a non-conventional NMF approach is needed in the form of a SSM, which facilitates the MMF (a method for finding the involved multiscale structure and the defining of the involved wavelets for a multi-resolution representation) [20] as well as, in turn, the determination of the MMF's CORWT, and the ensuing CWT.

C. MMF, CORWT, and Higher Resolution

MMF can adequately capture the matrix structure and varied scales. It is a convenient alternative to prevailing low-rank paradigms, such as Low-Rank Time-Frequency Structure (LRTFS), as the time-to-frequency transformation is reversible and the original SuT can be reconstructed by computing the Inverse Fourier Transform (IFT) [21, 22]). This should be of no surprise, as MMF is based on an approximate factorization of WT, as shown in equation (2):

$$WT \approx WT_1^T\, WT_2^T \ldots WT_2^T\, D\, WT_s WT_{s-1} WT_1, \tag{2}$$

where WT_j $(j = 1, \ldots, S)$ are sparse and orthogonal matrices, and D is close to the diagonal [23]. MMF's CORWT provides an enhanced time-frequency representation. As pertinent contextual information, whereas FT may suffice for stationary paradigms, and windowed FT may suffice for non-stationary paradigms, windowed FT is — axiomatically — constrained, as the size of the time-frequency window is fixed. In contrast, CORWT has a flexible time-frequency window (i.e., adjustable resolution) [24], and the pathway from MMF -> CORWT -> CWT are a core component of our Adaptive Resolution Transform (ART). The CORWT of the SuT, which segues to the ensuing CWT, lends well to generating scaleograms and time-frequency representations with higher resolution than STFT [25]. Hence, the amalgam of NMF and MMF are central to operationalizing this paper's posited implementation approach, and the pathway from NMF through CWT constitutes our ART. The hitherto RCR-based CLNN can now be expressed as an RCR-based CLNN-NMF/MMF construct, which is the engine that operationalizes our ART.

However, there are implementation challenges to obtaining CORWT, such as the fact that widely varying WT implementations (e.g., PyTorch, Python, C, etc.) pervade the code base ecosystem. In contrast to STFT (with its equally spaced time-frequency localization), WT provides high frequency resolution at low frequencies and high time resolution at high frequencies. In accordance with this fairly well-established characteristic, WT should be the favored pathway for the GHz range (despite the varied computational cost); this then segues to the implementation pathway of the WT onto the posited RCR-based CRT-CLNN-NMF/MMF construct.

The varied WT implementations necessitate scrutinization. By way of background information, as the WT is not time-invariant, supplanting the orthogonal WT with a translation-invariant WT (e.g., cycle-spinning, which compensates for the lack of shift invariance for the WT by averaging over the involved denoised, cyclically-shifted versions [26]), is crucial for the task at hand. Adhering to this described translation invariance within the involved perceptrons (the utilized algorithms for the supervised learning of the binary classifiers) is critical, and a translation-invariant linear operator can readily be represented as a convolutional operator. Moreover, the multiscale structure (i.e., relevant features are comprised of combinations of smaller features), such as discerned by MMF, segues to the preference of deeper cascade learning (i.e., cascades of predictors/classifiers), via ever smaller convolutional filters (thereby resembling WT). Overall, the RCR-based CRT-CLNN-NMF/MMF construct is quite well suited for translation-invariant WT implementations (i.e., as WTs provide acceptable SuT representation in the time-frequency plane and WTs are central for a constrained RCR-based CRT-CLNN input discernment feature, such as by optimally utilizing segments of the coefficients [27]). The RCR-based CRT-CLNN-NMF/MMF construct nicely accentuates the distinction between the WT proficiency in contending with nonstationary SuTs and singularities as contrasted to the Fourier proficiency of stationary SuTs (and associated global features). This proficiency is particularly

amplified when using Cross Wavelet Analysis (CWA). Given the varied time series $x(t_i)$ and $y(t_i)$ for the WoIs to be compared from the involved SuTs, discernment can be conducted via the wavelet coherency, which equates to the amplitude of the Wavelet Cross Spectrum (WCS) normalized to the involved Wavelet Power Spectrums (WPS), as shown in Equation 3.

$$WCS_i(s) = \frac{|\,WCS_i(s)\,|}{\sqrt{WPS1_i(s)\,WPS2_i(s)}} \tag{3}$$

There is yet another subtlety. By way of example, PyWavelets (a Python-based open-source WT library) contains Mother Wavelets (i.e., families of Wavelets, which encompass both DWT and CWT). Within each Wavelet family, there may be varied Wavelet subcategories. Generally, the subcategories are differentiated by the number of coefficients (i.e., the number of vanishing moments, which refers to the state wherein the Wavelet coefficients are zero for those polynomials with a degree of at most $p-1$, and the scaling function alone can be utilized to represent the function) as well as the level of decomposition. As the number of vanishing moments increases, the polynomial degree of the wavelet increases, and the involved graph becomes smoother. It turns out that the utilization of CWT enables the intricate structural characteristics of the SuT, within the transform space, to be better illuminated such that the set of WoIs are more amenable for analysis/discernment [28, 29]. The CWT is defined by Equation 4.

$$CWT\,(\alpha,\beta) = \int SuT(t)MW(t)dt\ = \frac{1}{\sqrt{\alpha}}\int SuT(t)MW_{\alpha}^{\gamma}\left(\frac{t-\beta}{\alpha}\right) \tag{4}$$
$$dt$$

where α is the scale factor, β is the translation factor, γ is the complex conjugate, and $MW(t)$ is the Mother Wavelet function [30]. To elaborate upon this aspect, and as a simple test, we take a chosen method of signal modulation (the encoding of information in a manner that is conducive for transmission), say, Multiple Frequency Shift Keying (MFSK), which is defined by Equation (5)

$$SuT_{MFSK}\,(t) = \sqrt{SuT_E}\,e^{ix[(\gamma+\delta_n)t+\,\varepsilon+\,\zeta_n]} \tag{5}$$

where SuT_E is the SuT energy, γ is the carrier frequency, δ is the frequency variation of the nth symbol, ε is the carrier initial phase, and ζ_n is the phase factor [31]. Substituting Equation 4 into Equation 3, we obtain Equation 6.

$$CWT_{MFSK}\,(\alpha,\beta) = e^{ix[(\gamma+\delta_n)\beta+\,\varepsilon+\,\zeta_n-\frac{\pi}{2}]} \tag{6}$$

The discernment enablement of CWT can be seen, and it is now apropos to be more explicit, and the hitherto RCR-based CRT-CLNN-NMF/MMF construct can now be expressed as an RCR-based CRT-CLNN-NMF/MMF-CWT discernment engine.

IV. Experimentation Findings

Sufficiently high resolution, particularly at the higher-order harmonics, is essential for waveform discernment in 5G/B5G/6G systems. Conventional approaches to classifying 5G/B5G/6G WoIs involve measurements under varied propagation conditions and blockage sensitivities. Analytical models, which consider the aforementioned conditions, and variations of directional beamforming have endeavored to contend with the challenges of waveform discernment. Our experimental RCR-based CRT-CLNN-NMF/MMF-CWT discernment engine leverages pre-computed hashes (which are assigned to each WoI previously encountered) and lookup table (which stores the pre-computed hashes) to facilitate incoming WoI classification and discernment in quasi-real-time. Regardless of the WoI, it can still be represented by a hash. Overall, the pre-computed hash and lookup table approach facilitates WoI classification and discernment.

Clearly, these higher dimensional representational vectors (i.e., hashes) have speed advantages over traditional representational approaches. After all, the deluge of SuTs and their associated WoI sets often leads to billions, trillions, or more vectors. By the utilization of hashes, the SuTs can be organized into overarching spatiotemporal Entities of Interest (EoI). The significance of this is as follows. EoIs within, say, a Dense Base Station Network (DBSN) are more likely to contain SuTs and their constituent WoIs of particular characteristics (given particular propagation conditions and blockages) than those EoIs within, say, a Sparse Base Station Network (SBSN). Accordingly, given a query vector, both the superset of EoIs and subsets of WoIs that are in closest proximity to the query vector (in terms of Euclidean distance) as well as those that have the highest dot product with the query vector, are returned for this "maximum inner-product" search query. The involved ontological structure is shown in Figure 2.

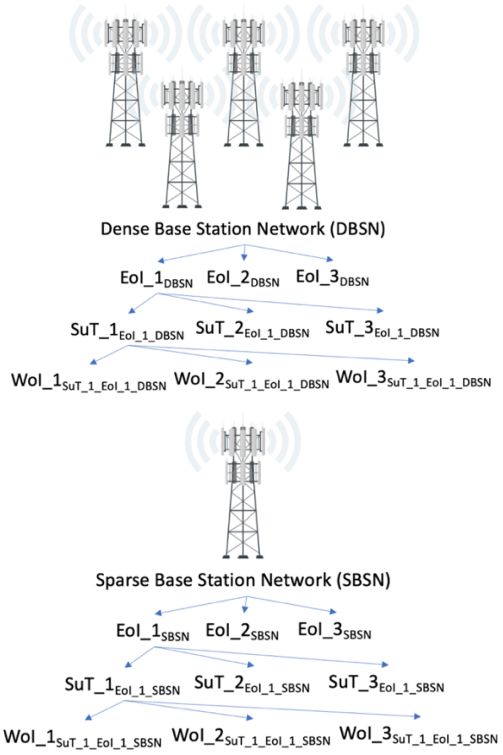

Fig. 2. DBSNs, SBSNs, EoIs, SuTs, and WoIs

A pre-indexing system, hereinafter known as a Pre-Indexing Module (PIM), containing known WoIs and their corresponding hashes, was utilized to facilitate quasi-real-time classification and discernment. The PIM undertakes classification into four core categories: (1) EOI_1, (2) EOI_2a, (3) EOI_2b, and (4) EOI_3. The WoIs in EOI_1 are "unlikely to be observed" (WoIs that occur infrequently). The WoIs in EOI_3 are "likely to be observed" (WoIs that occur frequently) on an ongoing basis. As further contextual information becomes available (e.g., the WoIs are found to be emanating from a DBSN as contrasted to a SBSN), some WoIs are further organized into EOI_2b, as the RCR-based CRT-CLNN-NMF/MMF-CWT discernment engine's PIM deems particular WoIs to have a similar morphology to those WoIs known to have emanated from a DBSN); extraneous background WoIs are further organized into EOI_2a. Pursuant to the involved classifiers, EOI_2a WoIs can be migrated to EOI_1, and EOI_2b WoIs can be migrated to EOI_3. Once the EOI_3-related WoI Observational Space Set (WoI_OSS) — the ascertained set of WoIs — is determined, the PIM determines the top candidates for the ensuing virtual scope rendering of the SA to facilitate the hybridized time-frequency mappings (those that appear similar, but are actually distinct and disparate) of the higher dimensional scaleogram (the spectrogram generated by the WT of a lower dimensional SuT). The PIM workflow progression is shown in Figure 3. Due to the fact that EOI_2a and EOI_3 serve as interim repositories, they are collectively referred to as a "Sandbox Data Lake."

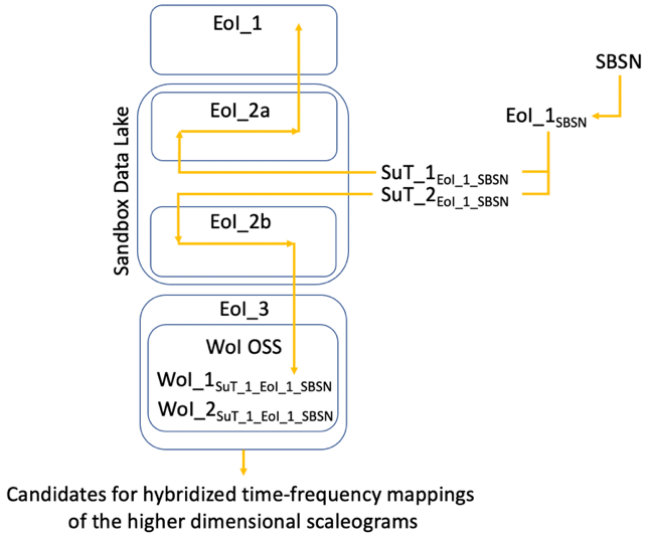

Fig. 3. RCR-CLNN-WT PIM workflow to obtain WoIOSS

Overall, the described elements can facilitate the discerning of anomalous aspects of high-frequency signals that may not otherwise be apparent. In fact, a wideband spectrogram (i.e., with an appropriately adjusted Fourier analysis window) can facilitate the discerning of adjacent individual harmonics, including at the higher-order harmonic level. Hence, the approach (by leveraging scaleograms) not only provides insight into the dynamic behavior of the SuT and encompassing system (including EOIs), but it can also be utilized to robustly discern among the involved WoIs.

Within the 5G/B5G/6G ecosystem, exemplar WoIs include Generalized Frequency Division Multiplexing (GFDM), Filter Bank Multicarrier (FBMC), Orthogonal Frequency Division Multiplexing (OFDM), Universal Filtered Multi-Carrier Modulation (UFMC), etc. In turn, there are variants of these waveform types. For example, FBMC has two principal variants: Quadrature Amplitude Modulation (QAM) and real valued Offset QAM (OQAM) (a.k.a. FBMC/OQAM). OFDM, which conjoins the advantages of QAM and Frequency Division Multiplexing (FDM), has an even greater number of variants. UFCM (a generalization of FBMC and OFDM) has greater variants still. Taking QAM as an example, to reflect the number of data bits transmitted per time interval (b/t), the form M-QAM (MQAM) is utilized; M represents the b/t. For example, 2-QAM is the simplest form of QAM (a.k.a. Quadrature Phase Shift Keying or QPSK). To reflect the modulation wherein the data bits select one of M Phase Shift versions of the carrier to transmit the data, the form M-PSK (MPSK) is utilized. The magnitude of a normalized MPSK is defined by Equation 7,

$$| CWT_{MPSK}(\alpha,\beta) | = \frac{4}{\gamma\sqrt{\alpha}} sin^2\left(\gamma\frac{\alpha}{4}\right) \quad (7)$$

and the magnitude of a normalized MQAM WT is defined by Equation 8,

$$| CWT_{MQAM}(\alpha,\beta) | = \frac{4}{\gamma\sqrt{\alpha}} sin^2\left(\gamma\frac{\alpha}{4}\right) \quad (8)$$

wherein, for both, it should be self-evident that discernment is not viable by comparing these forms [31]. However, the "Variance of the Upper Envelope" (VUE) as pertains to the magnitude of the WT of a normalized CWT_{MFSK} (hereinafter referred to as VUE_1) will be greater than that for CWT_{MPSK} or CWT_{MQAM}. In essence, whereas $| CWT_{MFSK}(\alpha,\beta) |$ is a multistep function, the other components of the equation are constant values [31]. Consequently, CWT_{MFSK} can be clustered separately from CWT_{MPSK} or CWT_{MQAM}. Then, similarly (and iteratively), the VUE of a normalized CWT_{MQAM} (hereinafter referred to as VUE_2) will be greater than that of the others in its cluster. In essence, VUE (VUE_1, VUE_2, …VUE_n) facilitates discernment.

Preliminary experimentation has confirmed the potentiality of the posited implementation pathway described in this paper. As the two key metrics for gauging the practicality of a particular SuT/WoI processing pathway centers upon resolution (either maintaining a prespecified resolution or adjusting the resolution to meet proscribed latency requirements) and latency (i.e., sufficient computational speed), those preliminary findings will be presented first in Table 1.

TABLE I. PROCESSING PATHWAY CHARACTERISTICS FOR VARIOUS WAVELET TRANSFORM TYPES

Wavelet Transform Type	Processing Pathway Characteristics		
	Sufficient Resolution	***Sufficient Speed***	***Comments***
CWT	✓	✓	Characteristics of enhanced resolution and speed
SWT	✓	×	Characteristics of overcompensation, which increases latency
DWT	×	✓	Characteristics of spectral leakage, which decreases resolution

As can be seen, CWT is the preferred wavelet transform type (as it has both the requisite resolution and speed) over SWT (which has a higher latency due to a propensity for overcompensation) and DWT (which has a lower resolution due to spectral leakage).

Further preliminary experimentation involved performance benchmarking a CWT implementation aboard various classes of neural networks known to accommodate CWT implementations: Artificial Neural Networks (ANNs), Deep Convolutional Generative Adversarial Network (DCGANs), and CLNNs. The preliminary findings, which were anticipated, are presented in Table 2.

TABLE II. PERFORMANCE BENCHMARKS FOR VARIOUS NEURAL NETWORK TYPES WITH CWT IMPLEMENTATIONS

Neural Network Type	Performance Benchmarks		
	Parameter Sharing/Optimal Number of Parameters to Learn/Best Fit Approximation	***Contextualizes Spatial and/or Temporal Information***	***Computational Speed***
CLNN	✓	✓	✓
RNN	✓	✓	×
ANN	×	×	×

As can be seen, CLNN (a particular class of CNN), exhibited superior performance over RNN and ANN with a CWT implementation. This was anticipated, as by employing a cascading set of ever smaller convolutional filters within an RCR architecture, the CLNN leverages deeper cascade learning, which nicely emulates CWTs.

Additional preliminary experimentation centered upon benchmarking NMF against other techniques, such as SVD; NMF had superior interpretation results. Likewise, other preliminary experimentation centered upon benchmarking MMF against other techniques, such as LRTFS; MMF had superior reversibility characteristics. Given the page limitations of this paper, more quantitative comparisons will be provided in a subsequent paper for future work.

V. CONCLUDING REMARKS AND FUTURE WORK

Time-frequency representations provide powerful and intuitive features for the analysis and comparison of the involved time series for SuTs and their constituent WoIs [15, 32]. The WT of a lower dimensional SuT results in a higher dimensional scaleogram, which is, in essence, the spectrogram generated by a WT. This can provide insight into, by way of example, not only the period of the largest oscillations, but also when these oscillations occurred. Hence, the scaleogram approach not only provides insight into the dynamic behavior of the SuT and encompassing system, but it can also be utilized to robustly discern among the various constituent WoIs (without the issues of truncation by fixed predetermined fixed window size approaches). After all, the RCR-based CRT-CLNN-NMF/MMF-CWT discernment engine, as a specifically architected CNN, nicely succeeds WTs since WTs provide acceptable SuT representation in the time-frequency plane by optimally using only segments of the coefficients [33, 34]). Preliminary experimentation, involving the bespoke RCR-based CRT-CLNN-NMF/MMF-CWT discernment engine, which utilized an amalgam of a non-conventional NMF (i.e., combining the utilization of more naturalistic nonnegative data vectors with an SSM approach) and MMF, indicates promise with regards to the classifying/baselining of WoIs (e.g., avoiding the loss of data) over time (for deep learning) for the ensuing more robust discernment of WoIs (by taking an alternative higher dimensionality representation pathway). This approach more fully captures the structure and content of the involved matrices so as to achieve higher resolution/discernment. Moreover, the CRT-CLNN-NMF/MMF-CWT discernment engine construct is well suited for the desired translation-invariant CWT PyWavelet numerical implementation aboard the involved CNN. The CWT PyWavelet is the preferred embodiment of the desired scaleograms for time series comparison. Consequently, the ART approach (NMF -> GCM -> SSM -> MMF -> CORWT -> CWT) well illuminates VUE and shows promise in facilitating the analysis/discernment of WoIs.

Future work will involve further refining the discernment engine architecture, such as by way of a particular treatment for the determination of the covariance matrix, which was previously addressed in [35]. For example, architecturally, to facilitate the requisite discernment, autodiff libraries (e.g., a C++ library that facilitate automatic differentiation of mathematical functions) are often utilized to enable large-scale tuning of a myriad of parameters defined by the involved numerical algorithm (e.g., https://github.com/pulver/autodiff), and the envisioned specialized workflow for refining the discernment engine architecture is comprised of enhancing the following: (1) iterative convolutions with ever smaller filters (wherein the filter depth is smaller than the input layer depth, such that kernel size is less than the channel size), (2) pointwise nonlinearities (which are relationships that are already equivariant to permutations of the input/output indices), and (3) constrained subsampling operations, such that, collectively, the resultant paradigm nicely bears semblance/emulates the WT (with complex normals — location parameter, relation matrix, and covariance matrix — at every scale) [36, 37].

ACKNOWLEDGMENT

The authors would like to thank Vit Tall and the University of Arizona for the collaborative framework pertaining to this 5G/B5G/6G-related white paper series. The authors would also like to acknowledge various organizations, such as ED2, for their encouragement related to advancing matters within the 5G/B5G/6G ecosystem.

REFERENCES

[1] W. Zhang, M. Feng, M. Krunz, and A. Abyaneh, "Signal detection and classification in shared spectrum: A deep learning approach," *Proc. of the IEEE INFOCOM 2021 Conference*, May 2021.

[2] Y. E. Sagduyu, T. Erpek, and Y. Shi, "Adversarial machine learning for 5G communications security," arXiv:2101.02656 [cs.NI].

[3] S. Chan, M. Krunz, and B. Griffin, "AI-based Robust Convex Relaxations for Supporting Diverse QoS in Next-Generation Wireless Systems," accepted for the IEEE ICDCS Workshop - Next-Generation Mobile Networking and Computing (NGMobile 2021), July 2021.

[4] S. Niar, O. Khan, and M. Tariq, "An Efficient Adaptive Window Size Selection Method for Improving Spectrogram Visualization," Computational Intelligence and Neuroscience, 2016, https://doi.org/10.1155/2016/6172453

[5] C. Zhao, M. He, and X. Zhao, "Analysis of transient waveform based on combined short time Fourier transform and wavelet transform," 2004 International Conference on Power System Technology, vol 2, 2004, pp. 1122-1126, doi: 10.1109/ICPST.2004.1460169.

[6] T. V. Aksenovich, "Comparison of the Use of Wavelet Transform and Short-Time Fourier Transform for the Study of Geomagnetically Induced Current in the Autotransformer Neutral," 2020 International Multi-Conference on Industrial Engineering and Modern Technologies, 2020, pp. 1-5, doi: 10.1109/FarEastCon50210.2020.9271210.

[7] C. Mateo and J. Talavera, "Bridging the gap between the short-time fourier Transfrom (STFT), wavelets, the constant-Q transform and multi-resolution STFT," Signal, Image and Video Processing, vol. 14, Nov 2020, pp. 1535-1543, doi: 10.1007/s11760-020-01701-8.

[8] W. Morsi and M. El-Hawary, "A new perspective for the IEEE standard 1459-2000 via stationary wavelet transform in the presence of nonstationary power quality disturbance," 2009 IEEE Power & Energy Society General Meeting, 2009, pp. 1-1, doi: 10.1109/PES.2009.5275160.

[9] T. Goktas, M. Zafarani, and B. Akin, "Discernment of broken magnet and static eccentricity faults in permanent magnet synchronous motors," IEEE Transactions on Energy Conversion, vol. 31, Jun 2016, pp. 578-587, doi: 10.1109/TEC.2015.2512602.

[10] I. I. Kosilina, "The Methods of Spectral Estimation of Signals Based on Kravchenko Weight Functions," 2007 International Kharkov Symposium Physics and Engrg. of Millimeter and Sub-Millimeter Waves, 2007, pp. 944-946, doi: 10.1109/MSMW.2007.4294869.

[11] "Windows and spectral leakage," Siemens. [Online]. Available: https://community.sw.siemens.com/s/article/windows-and-spectral-leakage

[12] S. Nittrouer, E. Tarr, T. Wicinich, A. Moberly, and J. Lowenstein, "Measuring the effects of spectral smearing and enhancement on speech recognition in noise for adults and children," J Acoust Soc Am, vol. 137, Apr 2015, doi: 10.1121/1.4916203.

[13] S. R. Konatham, L. R. Cortés, J. H. Chang, L. Rusch, S. LaRochelle and J. Azaña, "Photonic-Enabled Real-Time Frequency-Spectrum Tracking of Broadband Microwave Signals at a Nanosecond Scale," 2020 Optical Fiber Communications Conference and Exhibition, 2020, pp. 1-3.

[14] S. Konatham, R. Maram, L. Cortes, J. Chang, L. Rusch, S. LaRochelle, H. Chatellus, and J. Azana. "Real-time gap-free dynamic waveform spectral analysis with nanosecond resolutions through analog signal processing," Nature Communications, vol. 11, 2020, doi: 10.1038/s41467-020-17119-2.

[15] Andres Marafioti, N. Holighaus, N. Perraudin, and P. Majdak, "Adversarial generation of time-frequency features," Proceedings of Machine Learning Research, vol. 97, 2019, pp. 4352-4362.

[16] N. Gillis, "The why and how of nonnegative matrix factorization," Regularization, Optimization, Kernels, and Support Vector Machines, Jan 2014, pp. 257-291.

[17] A. Zaeemzadeh, M. Joneidi, B. Shahrasbi and N. Rahnavard, "Missing spectrum-data recovery in cognitive radio networks using piecewise constant Nonnegative Matrix Factorization," MILCOM 2015 - 2015 IEEE Military Communications Conference, 2015, pp. 238-243, doi: 10.1109/MILCOM.2015.7357449.

[18] R. Pentyala, "Variable length windowing to improve non-negative matrix factorization of music signals," MA, Ottawa-Carleton Institute for Electrical and Computer Engineering, Ottawa, ON, Canada, 2015. [Online]. Available: https://curve.carleton.ca/system/files/etd/1045aa1c-c200-45fa-b21b-2f39eb57ce48/etd_pdf/56a96571576512aa3c0563efa8a8d92f/pentyala-variablelengthwindowingtoimprovenonnegative.pdf

[19] C. Fevotte and M. Kowalski, "Low-rank time-frequency synthesis," Advances in Neural Information Processing Systems 27, 2014, pp. 1-9.

[20] R. Kondor, N. Teneva, P. Mudrakarta, "Parallel MMF: a multiresolution approach to matrix computation," Arxiv, 2015.

[21] "FFT (Fast Fourier Transform) Waveform Analysis," [Online]. Available: https://www.dataq.com/data-acquisition/general-education-tutorials/fft-fast-fourier-transform-waveform-analysis.html

[22] C Fevotte and M. Kowalski, "Estimation with low-rank time-frequency synthesis models," IEEE Transactions on Signal Processing, vol. 66, 2018, pp. 4121-4132, doi: 10.1109/TSP.2018.2844159.

[23] P. Mudrakarta and R. Kondor, "A generic multiresolution preconditioner for sparse symmetric systems," Jul 2017, doi: arXiv:1707.02054.

[24] V. Pukhova, E. Gorelova, G. Ferrini and S. Burnasheva, "Time-frequency representation of signals by wavelet transform," 2017 IEEE Conference of Russian Young Researchers in Electrical and Electronic Engineering 2017, pp. 715-718, doi: 10.1109/EIConRus.2017.7910658.

[25] Y. Zhang, Z. Guo, W. Wang, S. He, T. Lee, M. Loew, "A comparison of the wavelet and short-time fourier transforms for Doppler spectral analysis," Med Eng Phys, vol 25, Sep 2003, pp. 547-57, doi: 10.1016/S1350-4533(03)00052-3.

[26] "Translation invariant wavelet denoising with cycle spinning," [Online]. Available: https://www.mathworks.com/help/wavelet/ug/translation-invariant-wavelet-denoising-with-cycle-spinning.html

[27] A. Shteinberg, "Translation-invariant operators in Lorentz spaces," Funct Anal Its Appl, vol. 20, Dec 1986, pp. 166-168, doi: 10.1007/BF01077287.

[28] P. Addison, "Introduction to redundancy rules: the continuous wavelet transform comes of age," Philosophical Transaction of the Royal Society A., 2018, doi: https://doi.org/10.1098/rsta.2017.0258.

[29] A. Levinskis, "Convolution neural network feature reduction using wavelet transform," Electronics and Electrical Engineering, vol. 19, 2013, pp. 61-64, doi: 10.5755/j01.eee.19.3.3698.

[30] H. Liang and K. Ho, "Identification of digital modulation types using the wavelet transform," IEEE Military Communications. Conference Proceedings, 1999, pp. 427-431, doi: 10.1109/MILCOM.1999.822719.

[31] W. Li, Z. Dou, L. Qi, and C. Shi, "Wavelet transform based modulation classification for 5G and UAV communication in multipath fading channel," Physical Communication, June 2019, pp. 272-282. https://doi.org/10.1016/j.phycom.2018.12.019

[32] "FFT (Fast Fourier Transform) Waveform Analysis," [Online]. Available: https://www.dataq.com/data-acquisition/general-education-tutorials/fft-fast-fourier-transform-waveform-analysis.html

[33] A. Levinskis, "Convolution neural network feature reduction using wavelet transform," Electronics and Electrical Engineering, vol. 19, 2013, pp. 61-64, doi: 10.5755/j01.eee.19.3.3698.

[34] A. Akansu and R. Haddad, "Wavelet Transform," Multiresolution Signal Decomposition, Elsevier, 2001, doi: 10.1016/B978-0-12-047141-6.X5000-9.

[35] S. Chan, "Mitigation Factors for Multi-domain Resilient Networked Distributed Tessellation Communications," The Fifth International Conference on Cyber Technologies and Cyber-Systems, 2020, pp. 66-73, http://www.thinkmind.org/articles/cyber_2020_2_60_80061.pdf.

[36] C. Zhao, M. He, and X. Zhao, "Analysis of transient waveform based on combined short time Fourier transform and wavelet transform," 2004

International Conference on Power System Technology, vol 2, 2004, pp. 1122-1126, doi: 10.1109/ICPST.2004.1460169.

[37] J. Feydy, “From wavelet transforms to convolutional neural networks - part 2,” [Online]. Available: http://www.math.ens.fr/~feydy/Teaching/DataScience/cnn_part_2.html